ORIGINAL ARTICLE

Direct synthesis of mesoporous molecular sieves of Ni-SBA-16 by internal pH adjustment method and its performance for adsorption of toxic Brilliant Green dye

Asma Tufail Shah [a], **Muhammad Imran Din** [b,*], **Farva Nausheen Kanwal** [a], **Muhammad Latif Mirza** [c]

[a] Interdisciplinary Research Centre in Biomedical Materials, COMSATS Institute of Information Technology, Lahore 54000, Pakistan
[b] Institute of Chemistry, University of the Punjab, Lahore 54590, Pakistan
[c] Department of Chemistry, University of Sargodha, Pakistan

Abstract An ordered mesoporous novel material Ni-SBA-16 has been synthesized by internal pH-adjustment method. The synthesized material has been characterized by small angle XRD (SXRD), wide angle XRD (WXRD), Scanning Electron Microscope (SEM), High-Resolution Transmission Electron Microscope (HRTEM), Fourier-transform Infra-red (FTIR) spectroscope and Nitrogen Adsorption desorption techniques. The characterization results have shown that material possesses highly ordered mesostructure with high surface area (736 m^2/g) and large pore diameter (3.8 nm). FTIR and WXRD spectra revealed that nickel was uniformly dispersed on SBA-16 surface. The synthesized material has been used as adsorbent for removal of toxic Brilliant Green dye due to its large surface area and pore size. At optimized conditions, almost 100% of Brilliant Green dye was removed from aqueous solution by Ni-SBA-16. The isotherms analysis indicates that the Langmuir and Hill models provide the best correlation of the experimental data. The maximum adsorption capacity (q_{max}) of Ni-SBA-16 for Brilliant Green dye was 322.58 mg/g.

* Corresponding author. Tel.: +92 3007818870.
E-mail address: imrandin2007@gmail.com (M.I. Din).
Peer review under responsibility of King Saud University.

Production and hosting by Elsevier

1. Introduction

Ordered mesoporous molecular sieves have been focused as novel materials for many research areas like adsorption technology, molecular separation, catalysis, etc. (Lin et al., 2011; Wu et al., 2011; Yamauchi, 2013; Tang et al., 2014) In the last two decades a series of mesoporous SBA-type silica materials

such as SBA-15 (Lin et al., 2011), SBA-16 (Kresge et al., 1992; Zhao et al., 1998a,b; Rivera-Muñoz and Huirache-Acuña, 2010; da Silva et al., 2011; Kumar and Srinivas, 2012) and FDU-1 (Zhao et al., 1998b) with various structures have been synthesized by using triblock poly(ethylene oxide)–poly(alkylene oxide)–poly(ethylene oxide) copolymers as structure directing agents in strongly acidic medium (Sun et al., 2009; Cao and Kruk, 2011). Among these, SBA-16 is an environmental friendly material which possesses three dimensional cage like cubic Im3m structure with large surface area, pore diameter and dual-porosity system i.e., micropores and mesopores (Zhao et al., 1998b). These properties make these materials superior potential applicant for adsorption and catalysis applications (Sakamoto et al., 2000; Mesa et al., 2005). However, these purely siliceous materials are catalytically non-active because they have only silanol groups on their surface (Taguchi and Schuth, 2005; Shah et al., 2010). The substitution of heteroatoms (Ni^{2+}, Co^{2+}, Cu^{2+}, Al^{3+}, etc.) with valence lower than silicon generates acidity in these materials (Bottazzi et al., 2011; Dong et al., 2011; Shah et al., 2011). Nickel atom is considered an active and inexpensive metal in the chemical reactions and is being used in a variety of catalytic processes as a catalyst. The isomorphous substitution of heteroatom nickel for silicon in the structure of the mesoporous silica SBA-16 produces exchangeable sites which increases the adsorption of cationic dye Brilliant Green (Zanjanchi et al., 2007; Eftekhari et al., 2010). However, relatively few papers have been published on synthesis of nickel inside SBA-16 mesoporous materials (Cho et al., 2002). This is because the introduction of metal ions into the framework of SBA-16 by direct synthesis route is a difficult task due to the difficulties in the formation of M–O–Si (M = Ni) bond under the strong acidic conditions (Dong et al., 2011; Shah et al., 2011). Therefore there is a need to use the method which can result in maximum incorporation of nickel metal into silica framework.

Brilliant Green is an azo dye used in dyeing silk, wool, leather, jute and cotton. It is also used as a topical antiseptic and as a selective bacteriostatic agent in culture media (Hao et al., 2000; Janssen et al., 2003). Despite its widespread use, it is highly controversial material due to its serious effects on immune and reproductive systems and toxic properties which cause cancer, mutagenesis, teratogenicity and respiratory diseases (Mittal et al., 2008). Thus, it is of particular concern to remove Brilliant Green from wastewater in efficient and cost effective way before its release into the environment.

Here, in order to take the advantage of high surface area and large pore diameter of silica support and catalytic properties of nickel, Ni-SBA-16 has been synthesized by "internal pH-adjustment method" and used as adsorbent for removal of toxic Brilliant Green dye. Hexamethylene tetramine (HMTA) has been used as pH-modifier; it dissociates at high temperature to give ammonia, which increases the pH of the solution, as discussed previously (Cho et al., 2002). The synthesized material exhibited good adsorption ability. Equilibrium isotherms models have been applied for a better understanding of the adsorption process.

2. Experimental procedure

2.1. Materials

All solvents and reagents are commercially available and were used without further purification. Pluronic F127 and tetraethoxysilane were purchased from Sigma–Aldrich.

2.2. Synthesis of Ni-SBA-16

Ni-SBA-16 with Si/Ni molar ratio 36 (calculated from XRF) was prepared by internal pH adjustment method using $NiCl_2 \cdot 6H_2O$ as a source of nickel and HMTA as a complexing agent and internal pH-modifier. 2 g of pluronic F127 was dissolved in 100 mL of HCl solution (0.1 M) to get a clear solution. Then 9.5 g of tetraethyl orthosilicate (TEOS) was added drop-wise into this mixture. Then acidic solution of calculated amount of $NiCl_2 \cdot 6H_2O$ (Si/Ni molar ratios 40) and HMTA (HMTA/Ni molar ratio 1:1) was added into the above mixture. The final mixture was stirred for 20 h at RT (pH = 2) and transferred into a Teflon-lined stainless steel vessel, then placed in oven at 100 °C for 2 days. The resultant solid product was filtered, washed with distilled water, dried and calcined at 550 °C for 6 h (at heating rate of 1 °C/min). The actual Si/Ni molar ratio in synthesized sample was 36 (calculated from XRF analysis).

2.3. Adsorbate-Brilliant Green

The adsorbate, Brilliant Green (BG) dye (chemical formula = $C_{27}H_{34}N_2 O_4 S$, Molecular weight = 482.62, Solubility in water 100 g/L at 20 °C) was obtained from Sigma Aldrich (UK) (purity = 99.99%). The structure of Brilliant Green is illustrated in Fig. 1. Stock solution (1000 mg/L) of Brilliant Green dye was prepared by dissolving an accurately weighed amount of dye in double-distilled water.

2.4. Batch adsorption experiments

A series of experiments were carried out to study the effects of optimization parameters (adsorbent dose, pH, contact time and temperature) for adsorption of Brilliant Green dye on Ni-SBA-16. Stock solution (1000 mg/L) of Brilliant Green dye was prepared in deionized water and further diluted to get the desired concentration of dye. pH was adjusted with a digital pH meter (Jenway Model-3320) using 0.1 M HCl and 0.1 M NaOH solutions. Brilliant Green dye concentration for each experiment was found using a UV–Vis Spectrophotometer (Labomed Model-UVD3500, U.S.A) at λ_{max} 626 nm. For each experiment 50 ml of Brilliant Green dye solution of known concentration was used. For adsorption isotherms, Brilliant Green dye solutions of different known concentration
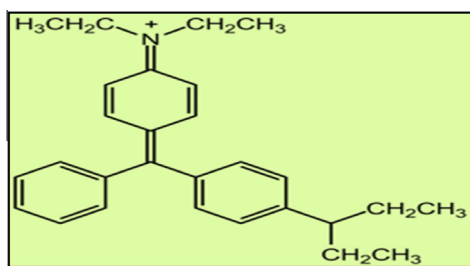

Figure 1   Structure of Brilliant Green Dye.

C_o were agitated with the known amount of adsorbent till the equilibrium was achieved. The kinetics of adsorption was determined by analyzing adsorptive uptake (q_t mg/g) of the dye from the aqueous solution at different time intervals. Effect of contact time on adsorption was studied in the range of 10–60 min with time interval of 10 min, the adsorbent dose of 0.5 g/50 mL and adsorbate concentration was 50 mg L^{-1}. All experiments were performed in triplicate and reported values are on average of three. The deviation was found to be 5% of the average value. The residual Brilliant Green dye concentration in the reaction mixture was analyzed by centrifuging the reaction mixture.

The percentage removal efficiency (R %) of adsorbent and uptake capacity at equilibrium q_e (mg/g)

$$(R \%) = \frac{C_o - C_e}{C_o} \times 100 \quad (1)$$

$$q_e(\text{mg/g}) = [C_o - C_e] \times \frac{V}{m} \quad (2)$$

where C_o is the initial dye concentration (mg/L), C_e is the concentration of Brilliant Green dye at equilibrium (mg/L). V is the volume of the solution in Liters and m is the mass of the adsorbent in grams.

3. Characterization techniques

X-ray powder diffraction (XRD) measurements were carried out with Rigaku D/Max 2500 VBZ+/PC diffractometer using Cu Kα radiation. The BET surface area of the samples was determined by the nitrogen adsorption isotherms using Quanta Chrome Autosorb-1-MP system. Before the nitrogen adsorption, each sample was pre-treated in vacuum at 200 °C for 3 h. The pore radius distribution was calculated from the desorption branch of the isotherm using Barrett–Joyner–Halenda (BJH) method. Scanning Electron Microscope (SEM) images were obtained by using Hitachi S-4700 microscope. High-Resolution Transmission Electron Microscope (HRTEM) images of samples were obtained on JEM-3010 transmission electron microscope. TEM samples were prepared by dispersing the Ni-SBA-16 in ethanol and dropping on sampling slide. The FT-IR spectra were recorded on a Bruker VECTOR 22 spectrometer in the range of 4000–400 cm^{-1}. The amount of nickel loaded on SBA-16 was calculated from Philips Magix-601 X-ray Fluorescence (XRF) spectrometer.

4. Results and discussion

4.1. Characterization of adsorbent material

The XRD spectra of Ni-SBA-16 sample are shown in Fig. 2a and b. The small angle XRD spectrum of Ni-SBA-16 exhibits a well-resolved strong diffraction peak (110) at 2θ value of about 0.69° (with d-spacing 12.2 nm), and comparatively unresolved peaks in the range of 1.0–2.0° indexed as (200) and (211) Bragg's reflections. The peaks are less pronounced due to the incorporation of nickel which may partially damage the pore structure (Liu et al., 2011). These peaks are associated with the body-centered cubic Im3m symmetry of three dimensional mesoporous structure of SBA-16. (Grudzien et al., 2007). The unit cell parameter (a_0) calculated from equation $a_0 = 2d110/3^{1/2}$ was 14 nm. These results show that the

mesostructure of SBA-16 is not higly affected during incorporation of heteroatom into its framework.

Wide-angle XRD pattern of the sample (Fig. 2b) shows a typical broad diffraction peak around 2θ value 24°, which is characteristic of amorphous silica. Absence of characteristic peak of crystalline NiO at 2θ value 36° and 45° shows that crystalline nickel was either absent or was not detectable due to low percentage (Liu et al., 2000). The actual Si/Ni molar ratio of the sample calculated from XRF (not shown here) was 36, which shows that most of the nickel was incorporated into the SBA-16 framework.

The SEM image of sample (Fig. 3a) shows that its morphology is not disturbed during incorporation of nickel into SBA-16 framework. No aggregation has been observed, which may reveal that nickel was uniformly distributed or no extra-framework nickel oxide was present. The homogeneity of the distribution of nickel and the ordering of the cubic array of mesoporous were examined by transmission electron microscopy. The transmission electron micrographs (Fig. 3b) of Ni-SBA-16 prepared by internal pH-adjustment method show the cubic array of uniform channels. The dark objects between the walls of SBA-16 may be nickel-oxide nanoparticles (Shah et al., 2007). SEM and TEM results reveal that nickel was successfully incorporated into silica without affecting its structural morphology and homogeneity to much extent.

Fig. 4a and b illustrates the Nitrogen physisorption isotherm of Ni-SBA-16, which exhibits type IV N$_2$ physisorption isotherm (according to IUPAC classification) with H2 hysteresis loop and a narrow pore size distribution curve which is characteristic of mesoporous materials with cage-type (Im3m) porous structure, similar to those found for SBA-16 (Grudzien et al., 2007; Meng et al., 2007; Shah et al., 2007; Zhu et al., 2010). The sharp pore size distribution curve is indicative of uniform mesoporous structure of the Ni-SBA-16 with average pore diameter 3.8 nm. The specific surface area of the sample was 736 m^2/g with pore volume 0.88 cm^3/g. Combining these data with the XRD results, the wall thickness, which was calculated by $w = 2d_{110}/3^{1/2} - D_p$ was 10.2 nm. Thus the introduction of heteroatom into silica spheres has not reduced the surface area to much extent compared to the conventional post pH adjustment method. The same results had been observed in our previous work for Cu-SBA-16 Grudzien et al., 2007.

Fig. 4c presents the FT-IR spectrum of calcined Ni-SBA-16 sample. The synthesized material shows three peaks at 465 cm^{-1}, 800 cm^{-1}, and 1085 cm^{-1} are corresponding to the rocking, bending (or symmetric stretching), and asymmetric stretching of the inter-tetrahedral oxygen atoms in SiO$_2$ of SBA-16, respectively (Cho et al., 2002; Kumar and Srinivas, 2012). Si–O–Si also gives a vibration absorption band at 1090 cm^{-1} which is assigned to ν_{as} (Si–O–Si). In synthesized sample this peak shifts to 1085, this shift of the absorption peaks toward the lower wave number is considered as an indication of metal incorporation into the framework of silica tetrahedral (Kadgaonkar et al., 2004). The band at ca. 964 cm^{-1} is attributed to the stretching vibration of SiO units bound to metal (nickel) atoms, but pure silica also gives such a band around 960 cm^{-1}. Thus, this band may be interpreted in terms of overlapping of both Si–OH and M–O–Si bond vibrations (Shah et al., 2011).

During pre-thermal steps the pH value is acidic (pH < 2), thus the structural integrity of SBA-16 is not affected. During
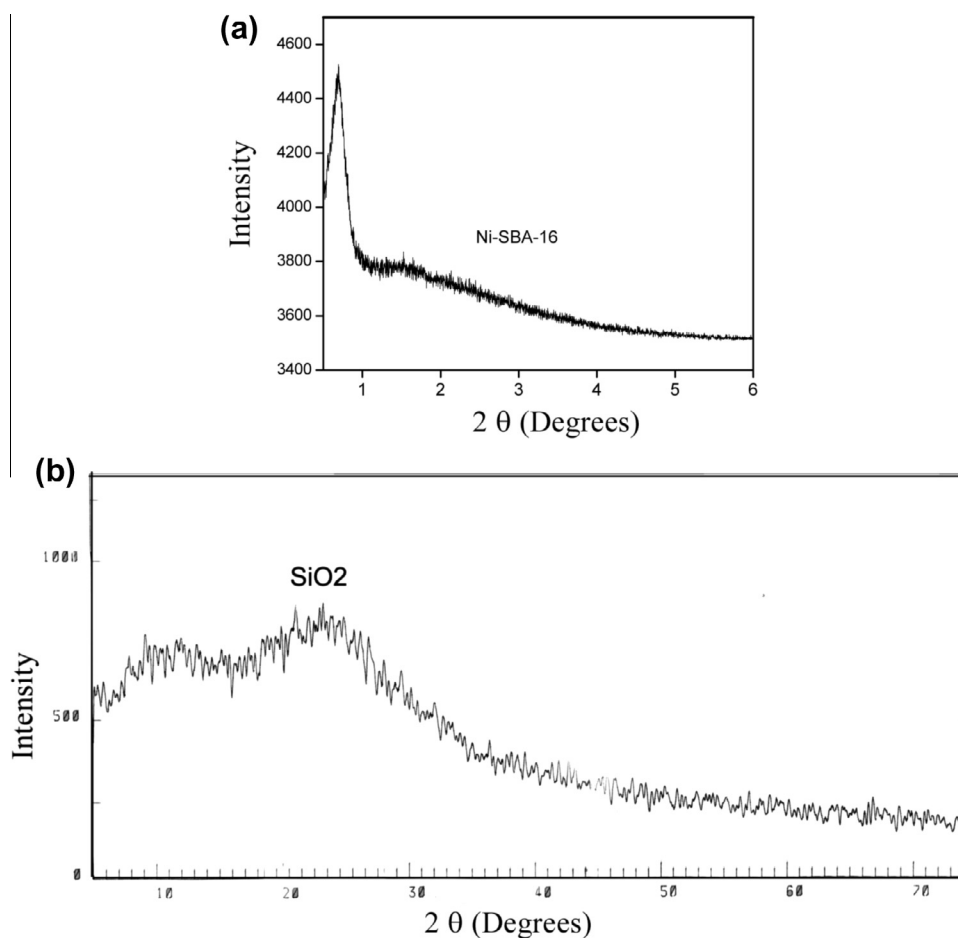
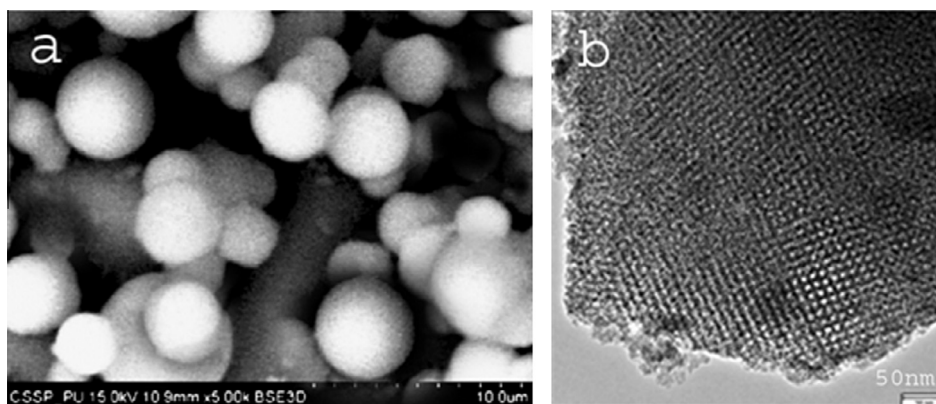**Figure 2**   (a) SXRD of Ni-SBA-16 sample. (b) WXRD of Ni-SBA-16 sample.

Figure 3   (a) SEM image of Ni-SBA-16. (b) HRTEM image of Ni-SBA-16 sample.

heating at 100 °C HMTA dissociates into NH_3 and HCHO, the ammonia increases the pH value of the gel to slightly alkaline, which leads to formation of Nickel oxo species and results in strong interaction between metal oxo species and silica.

Therefore, HMTA acts as an internal pH-modifier and helps to introduce more metal into SBA-16 framework without effecting its structural organization to much extent. HMTA also acts as a complexing agent by making a complex with metal ions, as discussed before (Shah et al., 2010).

4.2. Adsorption activity of Ni-SBA-16

Due to ordered mesostructure, high surface area, large pore diameter and high nickel contents Ni-SBA-16 has been used as an adsorbent for removal of toxic Brilliant Green dye from the aqueous medium, wherein it exhibited good adsorption activity. The adsorption kinetics of Brilliant Green dye onto Ni-SBA-16 was very fast, the equilibrium was attained after 25–30 min.
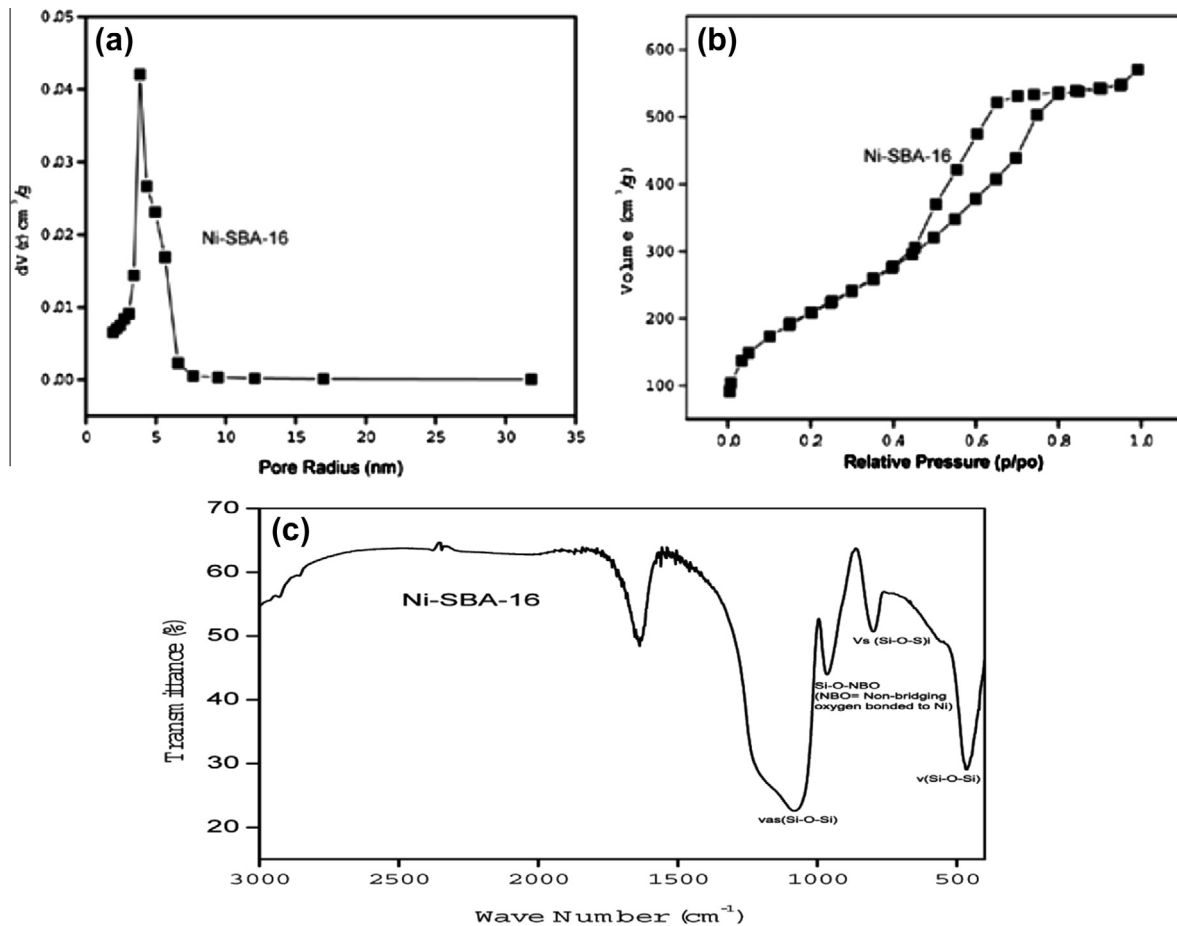
Figure 4 (a and b) N_2 physical adsorption and desorption isotherms and pore size distribution curve of Ni-SBA-16 sample. (c) FTIR spectrum of calcined Ni-SBA-16 sample.

4.3. Adsorption isotherms

The principle of adsorption isotherms is to find the relationship between the mass of the solute adsorbed per unit mass of adsorbent q_e (mg/g) and the solute concentration in the solution at equilibrium C_e (mg/L). Equilibrium isotherms were analyzed by Freundlich, Langmuir, Dubinin–Radushkevich (D–R), Redlich–Peterson and Hill isotherm models (Din and Mirza, 2013). Each isotherm model with their non-linear and linear form is given in Table 1. To find out the best fitting isotherm model nonlinear chi-square test (χ^2) was carried out.

4.3.1. Isotherm modeling

For adsorption isotherm parameters determination, the nonlinear method is preferred to the linear one. (Dhaouadi and M'Henni, 2009; Zakhama et al., 2011). All the model parameters were evaluated by non-linear regression using Excel 2007 software (Microsoft, USA). The optimization procedure requires a trial and error procedure to be defined in order to be able to evaluate the fit of the equation to the experimental data.

The nonlinear chi-square test (χ^2) is a statistical tool required for the best fit of an adsorption system, it is represented as

$$\chi^2 = \sum_{i=1}^{n} \frac{(q_{e,cal} - q_{e,means})^2}{q_{e,means}} \quad (3)$$

Table 1 Adsorption isotherms modeling for adsorption of BG dye on Ni-SBA-16.

Adsorption isotherm	Non-linear form	Isotherm parameters	
Langmuir isotherm	$q_e = \frac{K_L \cdot q_m \cdot C_e}{1 + K_L \cdot C_e}$	q_m (mg/g)	343.2
		K_L (L/mg)	1.333
		χ^2	0.451
Freundlich isotherm	$q_e = K_f C_e^{1/n}$	K_F	178.6
		n	4.09
		χ^2	1.69
(D–R) isotherm	$q_e = q_{DR} e^{-\beta \varepsilon^2}$	q_{DR} (mg/g)	306.6
		β	5.2×10^{-7}
		χ^2	1.62
Redlich–Peterson	$q_e = \frac{K_R \cdot C_e}{1 + a_R \cdot C_e^\beta}$	K_R	333.38
		a_R	0.674
		β	2.0
		χ^2	0.425
Hill	$q_e = \frac{q_{eH} \cdot C_e^{n_H}}{K_D + C_e^{n_H}}$	q_{eH} (mg/g)	319.31
		n_H	1.43
		K_D (L/mg)	0.549
		χ^2	0.421

Large value of (χ^2) indicates variation while its small value shows similarities of the experimental data (Ncibi, 2008).

The non-linear adsorption isotherm parameters (Fig. 5) are presented in Table 1.
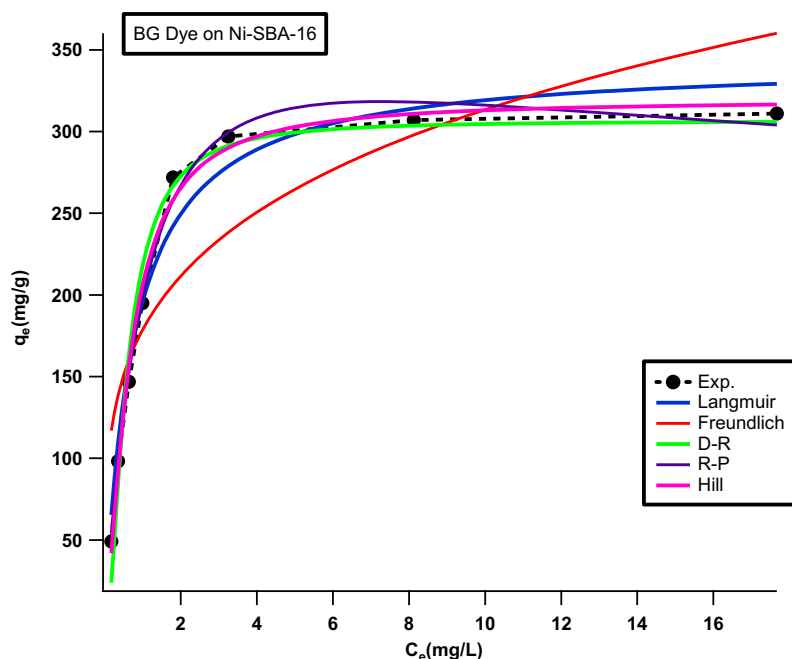
Figure 5   Non-linear adsorption isotherms plot for BG dye on Ni-SBA-16 at 50 °C; C_o = 50 mg/L; pH 1.0; Dose 0.01 g/50 mL; speed of agitation 125; t = 30 min.

Table 2   Comparison of adsorption performance of Ni-SBA-16 for removal of BG dye with some other adsorbents.

Adsorbent	q_{max} (mg/g)	Equilibrium time (min)	Equilibrium model	Kinetic model	Ref.
1. Saklıkent mud	1.18	150	Langmuir	PSO	Kismir and Aroguz (2011)
2. Acorn	2.11	30	Langmuir	PSO	Ghaedi et al. (2011)
3. CoFe$_2$O$_4$	3.58	60	Langmuir	FO	Zhang et al. (2008)
4. Rice husk ash	26.18	300	Langmuir and R–P	PSO	Mane et al. (2007a)
5. Modified Saw dust	58.47	180	R–P and Temkin	PSO	Mane and Babu (2011)
6. Kaolin	65.42	90	Langmuir	PSO	Nandi et al. (2009)
7. Bagasse fly ash	133.33	300	Langmuir and R–P	PSO	Mane et al. (2007b)
8. Ni-SBA-16	322.58	30	Langmuir and Hill	PSO	Present study

FO = first order, PFO = Pseudo first order, PSO = Pseudo second order, R–P = Redlich–Peterson.

Fig. 5 shows the relationship between experimental data and the predicted values by non-linear method. The Freundlich isotherm has high chi-square test (χ^2) values indicated that adsorption of Brilliant Green dye on Ni-SBA-16 did not follow Freundlich isotherm. It can be observed that among two parameters isotherms the adsorption of Brilliant Green on Ni-SBA-16 follow Langmuir isotherm, which indicates that the uptake occurs on a homogenous surface by monolayer adsorption. Low chi-square test (χ^2) value also favored Dubinin–Radushkevich isotherm model for this sorbate–sorbent system. A harmony has been found between the ratio K_R/a_R of the Redlich–Peterson model. Although Redlich–Peterson model has low value of chi-square (χ^2 = 0.425) But, the β value indicated that Redlich–Peterson model did not fit for the expression of adsorption of Brilliant Green dye on Ni-SBA-16 as the value of β (2.0) was much higher than unity (Brdar et al., 2012).

The Hill model correctly predicts the adsorption isotherms of Brilliant Green dye on Ni-SBA-16. The chi-square (χ^2) value was (0.421) less than Redlich–Peterson. On the basis of the chi-square (χ^2) values the Hill equation appears slightly preferable

than that of the Redlich–Peterson isotherm model (Din and Mirza, 2013).

4.4. Comparison of Ni-SBA-16 with other adsorbents

Ni-SBA-16 has been compared in terms of adsorption capacity, time of contact, Kinetic and equilibrium model. Table 2 shows such a comparison (Bhattacharyya and Sarma, 2003; Mane et al., 2007a,b; Zhang et al., 2008; Nandi et al., 2009; Ghaedi et al., 2011; Kismir and Aroguz, 2011; Mane and Babu, 2011). It can be easily observed that the adsorption capacity of Ni-SBA-16 is high as compared to a number of other materials. It also provides a shorter time of contact and indicates a faster removal of toxic Brilliant Green dye. So, it can be concluded that Ni-SBA-16 has potential for the removal of toxic Brilliant Green dye from aqueous solutions.

5. Conclusion

A novel material Ni-SBA-16 was prepared by internal pH-modification method using HMTA as an internal pH-modifier

and complexing agent. The synthesized material possesses uniform spherical morphology, large surface area and ordered mesostructure with high surface area (736 m^2/g). Ni-SBA-16 was proved to be an effective adsorbent for the adsorption of Brilliant Green dye from aqueous solution. Nearly 100% removal of dye was possible at a pH value of 1 under the batch test conditions. Equilibrium sorption data of Brilliant Green dye were best fitted to the Langmuir and Hill isotherms.

Acknowledgment

References

Bhattacharyya, K.G., Sarma, A., 2003. Adsorption characteristics of the dye, Brilliant Green, on Neem leaf powder. Dyes Pigments 57, 211–222.

Bottazzi, G.S.B., Martínez, M.L., Costa, M.B.G., Anunziata, O.A., Beltramone, A.R., 2011. Inhibition of the hydrogenation of tetralin by nitrogen and sulfur compounds over Ir/SBA-16. Appl. Catal. A 404, 30–38.

Brdar, M., Šćiban, M., Takači, A., Došenović, T., 2012. Comparison of two and three parameters adsorption isotherm for Cr(VI) onto Kraft lignin. Chem. Eng. J. 183, 108–111.

Cao, L., Kruk, M., 2011. Facile method to synthesize platelet SBA-15 silica with highly ordered large mesopores. J. Colloid Interface Sci. 361, 472–476.

Cho, Y.S., Park, J.C., Lee, B., Kim, Y., Yi, J., 2002. Preparation of mesoporous catalyst supported on silica with finely dispersed Ni particles. Catal. Lett. 81, 89–96.

da Silva, L.C.C., Infante, C.M.C., Lima, A.W.O., Cosentino, I.C., Fantini, M.C.A., Rocha, F.R.P., Masini, J.C., Matos, J.R., 2011. Immobilization of glucose oxidase enzyme (GOD) in large pore ordered mesoporous cage-like FDU-1 silica. J. Mol. Catal. B: Enzym. 70, 149–153.

Dhaouadi, H., M'Henni, F., 2009. Vat dye sorption onto crude dehydrated sewage sludge. J. Hazard. Mater. 164, 448–458.

Din, M.I., Mirza, M.L., 2013. Biosorption potentials of a novel green biosorbent Saccharum bengalense containing cellulose as carbohydrate polymer for removal of Ni (II) ions from aqueous solutions. Int. J. Biol. Macromol. 54, 99–108.

Dong, Y., Niu, X., Zhu, Y., Yuan, F., Fu, H., 2011. One-pot synthesis and characterization of Cu-SBA-16 mesoporous molecular sieves as an excellent catalyst for phenol hydroxylation. Catal. Lett. 141, 242–250.

Eftekhari, S., Habibi-Yangjeh, A., Sohrabnezhad, S., 2010. Application of AlMCM-41 for competitive adsorption of methylene blue and rhodamine B: thermodynamic and kinetic studies. J. Hazard. Mater. 178, 349–355.

Ghaedi, M., Hossainian, H., Montazerozohori, M., Shokrollahi, A., Shojaipour, F., Soylak, M., Purkait, M.K., 2011. A novel acorn based adsorbent for the removal of Brilliant Green. Desalination 281, 226–233.

Grudzien, R.M., Grabicka, B.E., Jaroniec, M., 2007. Adsorption studies of thermal stability of SBA-16 mesoporous silicas. Appl. Surf. Sci. 253, 5660–5665.

Hao, O.J., Kim, H., Chiang, P.-C., 2000. Decolorization of wastewater. Crit. Rev. Environ. Sci. Technol. 30, 449–505.

Janssen, P.A., Selwood, B.L., Dobson, S.R., Peacock, D., Thiessen, P.N., 2003. To dye or not to dye: a randomized, clinical trial of a triple dye/alcohol regime versus dry cord care. Pediatrics 111, 15–20.

Kadgaonkar, M.D., Laha, S.C., Pandey, R.K., Kumar, P., Mirajkar, S.P., Kumar, R., 2004. Cerium-containing MCM-41 materials as selective acylation and alkylation catalysts. Catal. Today 97, 225–231.

Kismir, Y., Aroguz, A.Z., 2011. Adsorption characteristics of the hazardous dye Brilliant Green on Saklıkent mud. Chem. Eng. J. 172, 199–206.

Kresge, C.T., Leonowicz, M.E., Roth, W.J., Vartuli, J.C., Beck, J.S., 1992. Ordered mesoporous molecular sieves synthesized by a liquid-crystal template mechanism. Nature 359, 710–712.

Kumar, A., Srinivas, D., 2012. Selective oxidation of cyclic olefins over framework Ti-substituted, three-dimensional, mesoporous Ti-SBA-12 and Ti-SBA-16 molecular sieves. Catal. Today 198, 59–68.

Lin, S., Shi, L., Ribeiro Carrott, M.M.L., Carrott, P.J.M., Rocha, J., Li, M.R., Zou, X.D., 2011. Direct synthesis without addition of acid of Al-SBA-15 with controllable porosity and high hydrothermal stability. Micropor. Mesopor. Mater. 142, 526–534.

Liu, X., Chun, C.M., Aksay, I.A., Shih, W.-H., 2000. Synthesis of mesostructured nickel oxide with silica. Ind. Eng. Chem. Res. 39, 684–692.

Liu, X., Wang, R., Xia, Y., He, Y., Zhang, T., 2011. LiCl-modified mesoporous silica SBA-16 thick film resistors as humidity sensor. Sens. Lett. 9, 698–702.

Mane, V.S., Babu, P.V.V., 2011. Studies on the adsorption of Brilliant Green dye from aqueous solution onto low-cost NaOH treated saw dust. Desalination 273, 321–329.

Mane, V.S., Deo Mall, I., Chandra Srivastava, V., 2007a. Kinetic and equilibrium isotherm studies for the adsorptive removal of Brilliant Green dye from aqueous solution by rice husk ash. J. Environ. Manage. 84, 390–400.

Mane, V.S., Mall, I.D., Srivastava, V.C., 2007b. Use of bagasse fly ash as an adsorbent for the removal of Brilliant Green dye from aqueous solution. Dyes Pigments 73, 269–278.

Meng, X., Lu, D., Tatsumi, T., 2007. Synthesis of mesoporous silica single crystal SBA-16 assisted by fluorinated surfactants with short carbon-chains. Micropor. Mesopor. Mater. 105, 15–23.

Mesa, M., Sierra, L., Patarin, J., Guth, J.-L., 2005. Morphology and porosity characteristics control of SBA-16 mesoporous silica. Effect of the triblock surfactant Pluronic F127 degradation during the synthesis. Solid State Sci. 7, 990–997.

Mittal, A., Kaur, D., Mittal, J., 2008. Applicability of waste materials – bottom ash and deoiled soya – as adsorbents for the removal and recovery of a hazardous dye, Brilliant Green. J. Colloid Interface Sci. 326, 8–17.

Nandi, B.K., Goswami, A., Purkait, M.K., 2009. Adsorption characteristics of Brilliant Green dye on kaolin. J. Hazard. Mater. 161, 387–395.

Ncibi, M.C., 2008. Applicability of some statistical tools to predict optimum adsorption isotherm after linear and non-linear regression analysis. J. Hazard. Mater. 153, 207–212.

Rivera-Muñoz, E.M., Huirache-Acuña, R., 2010. Sol gel-derived SBA-16 mesoporous material. Int. J. Mol. Sci. 11, 3069–3086.

Sakamoto, Y., Kaneda, M., Terasaki, O., Zhao, D., Kim, J.M., Stucky, G.D., Shin, H.J., Ryoo, R., 2000. Direct imaging of the pores and cages of three-dimensional mesoporous materials. Nature 408, 449–453.

Shah, P., Ramaswamy, A.V., Lazar, K., Ramaswamy, V., 2007. Direct hydrothermal synthesis of mesoporous Sn-SBA-15 materials under weak acidic conditions. Micropor. Mesopor. Mater. 100, 210–226.

Shah, A.T., Li, B., Abdalla, Z.E.A., 2010. Direct synthesis of Cu-SBA-16 by internal pH-modification method and its performance for adsorption of dibenzothiophene. Micropor. Mesopor. Mater. 130, 248–254.

Shah, A.T., Li, B., Nagra, S.A., 2011. Preparation and characterisation of copper-substituted SBA-16 type mesoporous materials by modified pH-adjusting method. Can. J. Chem. Eng. 89, 1288–1295.

Sun, H., Tang, Q., Du, Y., Liu, X., Chen, Y., Yang, Y., 2009. Mesostructured SBA-16 with excellent hydrothermal, thermal and mechanical stabilities: modified synthesis and its catalytic application. J. Colloid Interface Sci. 333, 317–323.

Taguchi, A., Schuth, F., 2005. Ordered mesoporous materials in catalysis. Micropor. Mesopor. Mater. 77, 1–45.

Tang, J., Liu, J., Torad, N.L., Kimura, T., Yamauchi, Y., 2014. Tailored design of functional nanoporous carbon materials toward fuel cell applications. Nano Today 9, 305–323.

Wu, K.C.-W., Jiang, X., Yamauchi, Y., 2011. New trend on mesoporous films: precise controls of one-dimensional (1D) mesochannels toward innovative applications. J. Mater. Chem. 21, 8934–8939.

Yamauchi, Y., 2013. Field-induced alignment controls of one-dimensional mesochannels in mesoporous materials. J. Ceram. Soc. Jpn. 121, 831–840.

Zakhama, S., Dhaouadi, H., M'Henni, F., 2011. Nonlinear modelisation of heavy metal removal from aqueous solution using Ulva lactuca algae. Bioresour. Technol. 102, 786–796.

Zanjanchi, M.A., Ebrahimian, A., Alimohammadi, Z., 2007. A spectroscopic study on the adsorption of cationic dyes into mesoporous AlMCM-41 materials. Opt. Mater. 29, 794–800.

Zhang, L., Su, M., Guo, X., 2008. Studies on the treatment of Brilliant Green solution by combination microwave induced oxidation with $CoFe_2O_4$. Sep. Purif. Technol. 62, 458–463.

Zhao, D., Feng, J., Huo, Q., Melosh, N., Fredrickson, G.H., Chmelka, B.F., Stucky, G.D., 1998a. Triblock copolymer syntheses of mesoporous silica with periodic 50 to 300 angstrom pores. Science 279, 548–552.

Zhao, D., Huo, Q., Feng, J., Chmelka, B.F., Stucky, G.D., 1998b. Nonionic triblock and star diblock copolymer and oligomeric surfactant syntheses of highly ordered, hydrothermally stable, mesoporous silica structures. J. Am. Chem. Soc. 120, 6024–6036.

Zhu, Y., Dong, Y., Zhao, L., Yuan, F., 2010. Preparation and characterization of mesoporous VOx/SBA-16 and their application for the direct catalytic hydroxylation of benzene to phenol. J. Mol. Catal. A: Chem. A: Chemical 315, 205–212.